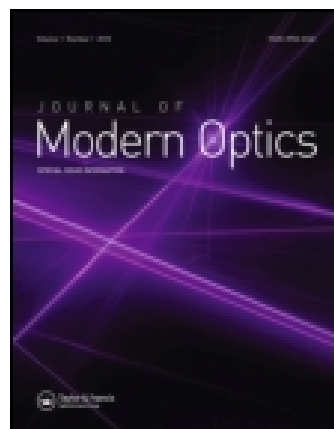


This article was downloaded by: [FU Berlin]

On: 30 April 2015, At: 23:21

Publisher: Taylor & Francis

Informa Ltd Registered in England and Wales Registered Number: 1072954 Registered office: Mortimer House, 37-41 Mortimer Street, London W1T 3JH, UK



## Journal of Modern Optics

Publication details, including instructions for authors and subscription information:

<http://www.tandfonline.com/loi/tmop20>

### Quantum theory of light diffraction

Xiang-Yao Wu<sup>a</sup>, Bai-Jun Zhang<sup>a</sup>, Jing-Hai Yang<sup>a</sup>, Li-Xin Chi<sup>a</sup>, Xiao-Jing Liu<sup>a</sup>, Yi-Heng Wu<sup>a</sup>, Qing-Cai Wang<sup>a</sup>, Yan Wang<sup>a</sup>, Jing-Wu Li<sup>b</sup> & Yi-Qing Guo<sup>c</sup>

<sup>a</sup> Institute of Physics, Jilin Normal University, Siping 136000, China

<sup>b</sup> Institute of Physics, Xuzhou Normal University, Xuzhou 221000, China

<sup>c</sup> Institute of High Energy Physics, PO Box 918(3), Beijing 100049, China

Published online: 14 Oct 2010.

To cite this article: Xiang-Yao Wu, Bai-Jun Zhang, Jing-Hai Yang, Li-Xin Chi, Xiao-Jing Liu, Yi-Heng Wu, Qing-Cai Wang, Yan Wang, Jing-Wu Li & Yi-Qing Guo (2010) Quantum theory of light diffraction, Journal of Modern Optics, 57:20, 2082-2091, DOI: [10.1080/09500340.2010.521593](https://doi.org/10.1080/09500340.2010.521593)

To link to this article: <http://dx.doi.org/10.1080/09500340.2010.521593>

PLEASE SCROLL DOWN FOR ARTICLE

Taylor & Francis makes every effort to ensure the accuracy of all the information (the "Content") contained in the publications on our platform. However, Taylor & Francis, our agents, and our licensors make no representations or warranties whatsoever as to the accuracy, completeness, or suitability for any purpose of the Content. Any opinions and views expressed in this publication are the opinions and views of the authors, and are not the views of or endorsed by Taylor & Francis. The accuracy of the Content should not be relied upon and should be independently verified with primary sources of information. Taylor and Francis shall not be liable for any losses, actions, claims, proceedings, demands, costs, expenses, damages, and other liabilities whatsoever or howsoever caused arising directly or indirectly in connection with, in relation to or arising out of the use of the Content.

This article may be used for research, teaching, and private study purposes. Any substantial or systematic reproduction, redistribution, reselling, loan, sub-licensing, systematic supply, or distribution in any form to anyone is expressly forbidden. Terms & Conditions of access and use can be found at <http://www.tandfonline.com/page/terms-and-conditions>

## Quantum theory of light diffraction

Xiang-Yao Wu<sup>a\*</sup>, Bai-Jun Zhang<sup>a</sup>, Jing-Hai Yang<sup>a</sup>, Li-Xin Chi<sup>a</sup>, Xiao-Jing Liu<sup>a</sup>, Yi-Heng Wu<sup>a</sup>,  
Qing-Cai Wang<sup>a</sup>, Yan Wang<sup>a</sup>, Jing-Wu Li<sup>b</sup> and Yi-Qing Guo<sup>c</sup>

<sup>a</sup>Institute of Physics, Jilin Normal University, Siping 136000, China; <sup>b</sup>Institute of Physics, Xuzhou Normal University, Xuzhou 221000, China; <sup>c</sup>Institute of High Energy Physics, PO Box 918(3), Beijing 100049, China

(Received 23 March 2010; final version received 31 August 2010)

At present, the theory of light diffraction only has the simple wave-optical approach. In this paper, we study light diffraction with the relativistic quantum theory approach. We find that the slit length, slit width, slit thickness and wavelength of light affect the diffraction intensity and form of diffraction pattern. However, the effect of slit thickness on the diffraction pattern cannot be explained by wave-optical approach, but it can be explained in quantum theory. We compare the theoretical results with single- and multiple-slits experimental data, and find the theoretical results are in accordance with the experimental data. In addition, we give some theory predictions. We think all new predictions will be tested by the light diffraction experiment.

**Keywords:** quantum theory; light diffraction

### 1. Introduction

It is known that the non-classical phenomena of two photon interference [1] and two-photon ghost diffraction and imaging [2,3] have classical counterparts. The classical two-photon interference of light was first discovered in the pioneering experiments by Hanbury Brown and Twiss [4] and since then it has been observed with various sources, including pseudo-thermal ones [5], true thermal ones [6], and coherent ones [7]. Somewhat later, ghost imaging with classical light was demonstrated, both in the near-field and far-field domains [8–10]. The present optical imaging technologies, such as optical lithography, have reached a spatial resolution in the sub-micrometer range, which comes up against the diffraction limit due to the wavelength of light. However, the guiding principle of such technology is still based on the classical diffraction theory established by Fresnel, Kirchhoff and others more than a hundred years ago. Recently, the use of quantum-correlated photon pairs (biphotons) to overcome the classical diffraction limit was proposed and attracted much attention. Obviously, quantum theory approaches are necessary to explain the diffraction-interference of the quantum-correlated multi-photon state. As is well known, Huygens' and Kirchhoff's theory, has been successfully applied to classical optics, and has yielded good agreement with many experiments. However, light interference and diffraction are quantum phenomena, and their full

description needs a quantum theory approach. In 1924, Epstein and Ehrenfest first studied light diffraction with the old quantum theory, i.e. the quantum mechanics of the correspondence principle, and obtained a result identical to that obtained using classical optics [11]. Here, in this work, we study the single-slit and multiple-slit diffraction of light from the relativistic quantum theory of photons approach. In view of quantum theory, the light has the nature of a wave, and the wave is described by the wave function. As the wave equation we study has the character of a vector, we choose wave function  $\vec{\psi}(\vec{r}, t)$  to describe the wave. The wave function  $\vec{\psi}(\vec{r}, t)$  can be calculated with a relativistic wave equation and it also has a statistical meaning, i.e.  $|\vec{\psi}(\vec{r}, t)|^2$  can be explained as the photon's probability density at the definite position. In light diffraction, because the diffraction intensity  $I$  is directly proportional to  $|\vec{\psi}(\vec{r}, t)|^2$ , we can obtain the diffraction intensity by calculating the light wave function  $\vec{\psi}(\vec{r}, t)$  distributed on the display screen, and the light wave functions can be divided into three areas. The first area is the incident area, where the photon wave function is a plane wave. The second area is the slit area, where the light wave function can be calculated by the quantum wave equation of light. The third area is the diffraction area, where the light wave function can be calculated by Kirchhoff's law. For multiple-slit diffraction, we can obtain the total diffraction wave function by the superposition of the

\*Corresponding author. Email: wuxy2066@163.com

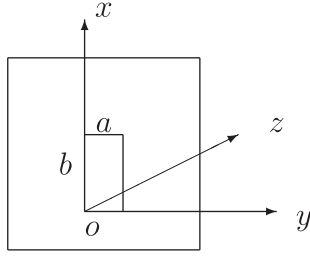


Figure 1. The single-slit geometry,  $a$  is the width and  $b$  is the length of the slit.

diffraction wave function of every slit. In the following, we will calculate these wave functions.

The paper is organized as follows. In Section 2 we calculate the light wave function in the single-slit with the quantum theory approach. In Section 3 we calculate the light wave function in the diffraction area with Kirchhoff's law. Section 4 is the multiple-slit diffraction wave function. Section 5 is the numerical result. Section 6 is a summary of results and the conclusions.

## 2. Quantum approach of light single-slit diffraction

In an infinite plane, we consider a single-slit, its width  $a$  and length  $b$  are shown in Figure 1. The  $x$ -axis is along the slit length and the  $y$ -axis is along the slit width. In the following, we calculate the light wave function in the single-slit with a relativistic wave equation. At time  $t$ , we suppose that the incident plane wave travels along the  $z$  axis. It is

$$\begin{aligned}\vec{\psi}_0(z, t) &= \vec{A} e^{\frac{i}{\hbar}(pz - Et)} \\ &= \sum_j A_j \cdot e^{\frac{i}{\hbar}(pz - Et)} \vec{e}_j \\ &= \sum_j \psi_{0j} \cdot e^{-\frac{i}{\hbar}Et} \vec{e}_j,\end{aligned}\quad (1)$$

where  $\psi_{0j} = A_j \cdot e^{\frac{i}{\hbar}pz}$ ,  $j = x, y, z$  and  $\vec{A}$  is a constant vector. The time-dependent relativistic wave equation of light is [12]

$$i\hbar \frac{\partial}{\partial t} \vec{\psi}(\vec{r}, t) = c\hbar \nabla \times \vec{\psi}(\vec{r}, t) + V\vec{\psi}(\vec{r}, t), \quad (2)$$

where  $c$  is light velocity. From Equation (2), we can find the light wave function  $\vec{\psi}(\vec{r}, t) \rightarrow 0$  when  $V(\vec{r}) \rightarrow \infty$ . The potential energy of light in the single-slit is

$$\begin{aligned}V(x, y, z) &= 0 \quad 0 \leq x \leq b, \quad 0 \leq y \leq a, \quad 0 \leq z \leq c' \\ &= \infty \quad \text{otherwise,}\end{aligned}\quad (3)$$

where  $c'$  is the slit thickness. We can get the time-dependent relativistic wave equation in the slit ( $V(x, y, z) = 0$ ), it is

$$i\hbar \frac{\partial}{\partial t} \vec{\psi}(\vec{r}, t) = c\hbar \nabla \times \vec{\psi}(\vec{r}, t), \quad (4)$$

by derivation of Equation (4) about time  $t$  and multiplying both sides by  $i\hbar$ , we have

$$(i\hbar)^2 \frac{\partial^2}{\partial t^2} \vec{\psi}(\vec{r}, t) = c\hbar \nabla \times i\hbar \frac{\partial}{\partial t} \vec{\psi}(\vec{r}, t). \quad (5)$$

Substituting Equation (4) into Equation (5), we have

$$\frac{\partial^2}{\partial t^2} \vec{\psi}(\vec{r}, t) = -c^2 [\nabla(\nabla \cdot \vec{\psi}(\vec{r}, t)) - \nabla^2 \vec{\psi}(\vec{r}, t)], \quad (6)$$

where the formula  $\nabla \times \nabla \times \vec{B} = \nabla(\nabla \cdot \vec{B}) - \nabla^2 \vec{B}$ . From [11], the photon wave function is  $\vec{\psi}(\vec{r}, t) = \sqrt{\frac{\epsilon_0}{2}}(\vec{E}(\vec{r}, t) + i\sigma c \vec{B}(\vec{r}, t))$ , we have

$$\nabla \cdot \vec{\psi}(\vec{r}, t) = 0, \quad (7)$$

from Equations (6) and (7), we have

$$\left(\frac{\partial^2}{\partial t^2} - c^2 \nabla^2\right) \vec{\psi}(\vec{r}, t) = 0. \quad (8)$$

Equation (8) is the same as the classical wave equation of light. Here, it is a quantum wave equation of light, since it is obtained from the relativistic wave Equation (2), and it satisfied the new quantum boundary condition: when  $\vec{\psi}(\vec{r}, t) \rightarrow 0$ ,  $V(\vec{r}) \rightarrow \infty$ . It is different from the classical boundary condition.

When the photon wave function  $\vec{\psi}(\vec{r}, t)$  changes with determinate frequency  $\omega$ , the wave function of photon can be written as

$$\vec{\psi}(\vec{r}, t) = \vec{\psi}(\vec{r}) e^{-i\omega t}. \quad (9)$$

Substituting Equation (9) into Equation (8), we can get

$$\frac{\partial^2 \vec{\psi}(\vec{r})}{\partial x^2} + \frac{\partial^2 \vec{\psi}(\vec{r})}{\partial y^2} + \frac{\partial^2 \vec{\psi}(\vec{r})}{\partial z^2} + \frac{4\pi^2}{\lambda^2} \vec{\psi}(\vec{r}) = 0, \quad (10)$$

and the wave function satisfies boundary conditions

$$\vec{\psi}(0, y, z) = \vec{\psi}(b, y, z) = 0, \quad (11)$$

$$\vec{\psi}(x, 0, z) = \vec{\psi}(x, a, z) = 0. \quad (12)$$

The photon wave function  $\vec{\psi}(\vec{r})$  can be written

$$\begin{aligned}\vec{\psi}(\vec{r}) &= \psi_x(\vec{r}) \vec{e}_x + \psi_y(\vec{r}) \vec{e}_y + \psi_z(\vec{r}) \vec{e}_z \\ &= \sum_{j=x, y, z} \psi_j(\vec{r}) \vec{e}_j,\end{aligned}\quad (13)$$

where  $j$  is  $x$ ,  $y$  or  $z$ . Substituting Equation (13) into Equations (10), (11) and (12), we have the component equation

$$\frac{\partial^2 \psi_j(\vec{r})}{\partial x^2} + \frac{\partial^2 \psi_j(\vec{r})}{\partial y^2} + \frac{\partial^2 \psi_j(\vec{r})}{\partial z^2} + \frac{4\pi^2}{\lambda^2} \psi_j(\vec{r}) = 0. \quad (14)$$

$$\psi_j(0, y, z) = \psi_j(b, y, z) = 0, \quad (15)$$

$$\psi_j(x, 0, z) = \psi_j(x, a, z) = 0. \quad (16)$$

The partial differential Equation (14) can be solved by the method of separation of variables.

$$\psi_j(x, y, z) = X_j(x)Y_j(y)Z_j(z). \quad (17)$$

From Equations (14), (15), (16) and (17), we can get the general solution of Equation (14)

$$\psi_j(x, y, z) = \sum_{mn} D_{mnj} \sin \frac{n\pi x}{b} \sin \frac{m\pi y}{a} e^{i\sqrt{\frac{4\pi^2}{\lambda^2} - \frac{n^2\pi^2}{b^2} - \frac{m^2\pi^2}{a^2}} z}, \quad (18)$$

since the wave functions are continuous at  $z=0$ , we have

$$\vec{\psi}_0(x, y, z; t) |_{z=0} = \vec{\psi}(x, y, z; t) |_{z=0}, \quad (19)$$

or, equivalently,

$$\psi_{0j}(x, y, z) |_{z=0} = \psi_j(x, y, z) |_{z=0} \cdot (j = x, y, z). \quad (20)$$

From Equations (1), (18) and (20), we obtain the coefficient  $D_{mnj}$  by Fourier transform

$$\begin{aligned} D_{mnj} &= \frac{4}{ab} \int_0^a \int_0^b A_j \sin \frac{n\pi\xi}{b} \sin \frac{m\pi\eta}{a} d\xi d\eta \\ &= \frac{16A_j}{mn\pi^2} m, n, \text{ odd} \\ &= 0 \text{ otherwise, } (j = x, y, z) \end{aligned} \quad (21)$$

substituting Equation (21) into Equation (18), we have

$$\begin{aligned} \psi_j(x, y, z) &= \sum_{m,n=0}^{\infty} \frac{16A_j}{(2m+1)(2n+1)\pi^2} \sin \frac{(2n+1)\pi x}{b} \\ &\quad \times \sin \frac{(2m+1)\pi y}{a} \\ &\quad \times e^{i\sqrt{\frac{4\pi^2}{\lambda^2} - \frac{(2n+1)^2\pi^2}{b^2} - \frac{(2m+1)^2\pi^2}{a^2}} z}, \quad (j = x, y, z) \end{aligned} \quad (22)$$

and substituting Equation (22) into Equations (9) and (13), we can obtain the photon wave function

in the slit

$$\begin{aligned} \vec{\psi}(x, y, z; t) &= \sum_{j=x,y,z} \psi_j(x, y, z, t) \vec{e}_j \\ &= \sum_{j=x,y,z} \sum_{m,n=0}^{\infty} \frac{16A_j}{(2m+1)(2n+1)\pi^2} \\ &\quad \times \sin \frac{(2n+1)\pi x}{b} \sin \frac{(2m+1)\pi y}{a} \\ &\quad \times e^{i\sqrt{\frac{4\pi^2}{\lambda^2} - \frac{(2n+1)^2\pi^2}{b^2} - \frac{(2m+1)^2\pi^2}{a^2}} z} e^{-i\omega t} \vec{e}_j. \end{aligned} \quad (23)$$

We can consider the case of a limit, i.e. the slit length  $b$  is infinity, and the Equations (8) and (10) become

$$\frac{\partial^2}{\partial t^2} \vec{\psi}(y, z, t) - c^2 \left( \frac{\partial^2}{\partial y^2} + \frac{\partial^2}{\partial z^2} \right) \vec{\psi}(y, z, t) = 0, \quad (24)$$

$$\frac{\partial^2 \vec{\psi}(y, z)}{\partial y^2} + \frac{\partial^2 \vec{\psi}(y, z)}{\partial z^2} + \frac{4\pi^2}{\lambda^2} \vec{\psi}(y, z) = 0, \quad (25)$$

we can easily obtain the light wave function in the single-slit when  $b \rightarrow \infty$

$$\begin{aligned} \vec{\psi}(y, z; t) &= \sum_{j=y,z} \psi_j(x, y, z, t) \vec{e}_j \\ &= \sum_{j=y,z} \sum_{m=0}^{\infty} \frac{4A_j}{(2m+1)\pi} \sin \frac{(2m+1)\pi y}{a} \\ &\quad \times e^{i\sqrt{\frac{4\pi^2}{\lambda^2} - \frac{(2m+1)^2\pi^2}{a^2}} z} e^{-i\omega t} \vec{e}_j. \end{aligned} \quad (26)$$

### 3. The wave function of light diffraction

In Section 2, we calculated the photon wave function in the slit. In the following, we will calculate the diffraction wave function. We can calculate the wave function in the diffraction area. From the slit wave function component  $\psi_j(\vec{r}, t)$ , we can calculate its diffraction wave function component  $\Phi_j(\vec{r}, t)$  by Kirchhoff's law. It can be calculated by the formula [13]

$$\Phi_j(\vec{r}, t) = -\frac{1}{4\pi} \int_{s_0} \frac{e^{ikr}}{r} \vec{n} \cdot \left[ \nabla' \psi_j + \left( ik - \frac{1}{r} \right) \frac{\vec{r}}{r} \psi_j \right] ds. \quad (27)$$

The total diffraction wave function is

$$\vec{\Phi}(\vec{r}, t) = \sum_{j=x,y,z} \Phi_j(\vec{r}, t) \vec{e}_j, \quad (28)$$

the diffraction area is shown in Figure 2, where  $k = \frac{2\pi}{\lambda}$  is the wave vector,  $s_0$  is the area of the single-slit,  $\vec{r}'$  is the position of a point on the surface ( $z = c'$ ),  $P$  is an arbitrary point in the diffraction area, and the  $\vec{n}$  is a

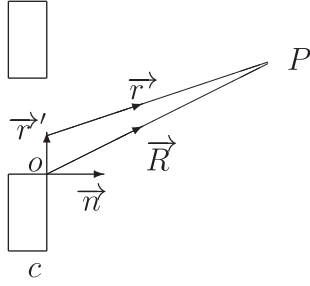


Figure 2. The diffraction area of single-slit.

unit vector, which is normal to the surface of the single-slit. From Figure 2, we have

$$\begin{aligned} r &= R - \frac{\vec{R}}{R} \cdot \vec{r}' \\ &\approx R - \frac{\vec{r}}{r} \cdot \vec{r}' \\ &= R - \frac{\vec{k}_2}{k} \cdot \vec{r}', \end{aligned} \quad (29)$$

then,

$$\begin{aligned} \frac{e^{ikr}}{r} &= \frac{e^{ik(R - \frac{\vec{r}}{r} \cdot \vec{r}')}}{R - \frac{\vec{r}}{r} \cdot \vec{r}'} \\ &\approx \frac{e^{ikR} e^{-i\vec{k}_2 \cdot \vec{r}'}}{R} (|\vec{r}'| \ll R), \end{aligned} \quad (30)$$

where  $\vec{k}_2 = k \frac{\vec{r}}{r}$ . Substituting Equations (22), (29) and (30) into Equation (27), one can obtain

$$\begin{aligned} \Phi_j(\vec{r}, t) &= -\frac{e^{ikR}}{4\pi R} e^{-i\omega t} \int_{s_0} e^{-i\vec{k}_2 \cdot \vec{r}'} \\ &\times \sum_{m=0}^{\infty} \sum_{n=0}^{\infty} \frac{16A_j}{(2m+1)(2n+1)\pi^2} \\ &\times e^{i\sqrt{\frac{4\pi^2}{\lambda^2} - \left(\frac{(2n+1)\pi}{b}\right)^2 - \left(\frac{(2m+1)\pi}{a}\right)^2} \cdot c'} \sin \frac{(2n+1)\pi}{b} \\ &\times x' \sin \frac{(2m+1)\pi}{a} y' \\ &\times \left[ i\sqrt{\frac{4\pi^2}{\lambda^2} - \left(\frac{(2n+1)\pi}{b}\right)^2 - \left(\frac{(2m+1)\pi}{a}\right)^2} \right. \\ &\left. + i\vec{n} \cdot \vec{k}_2 - \frac{\vec{n} \cdot \vec{R}}{R^2} \right] dx' dy'. \end{aligned} \quad (31)$$

Assume that the angle between  $\vec{k}_2$  and the  $x$  axis ( $y$  axis) is  $\frac{\pi}{2} - \alpha$  ( $\frac{\pi}{2} - \beta$ ), and  $\alpha(\beta)$  is the angle between  $\vec{k}_2$  and the surface of  $yz$  ( $xz$ ), then we have

$$k_{2x} = k \sin \alpha, \quad k_{2y} = k \sin \beta, \quad (32)$$

$$\vec{n} \cdot \vec{k}_2 = k \cos \theta, \quad (33)$$

where  $\theta$  is the angle between  $\vec{k}_2$  and the  $z$  axis. Substituting Equations (32) and (33) into Equation (31) gives

$$\begin{aligned} \Phi_j(x, y, z; t) &= -\frac{e^{ikR}}{4\pi R} e^{-i\omega t} \sum_{m=0}^{\infty} \sum_{n=0}^{\infty} \frac{16A_j}{(2m+1)(2n+1)\pi^2} \\ &\times e^{i\sqrt{\frac{4\pi^2}{\lambda^2} - \left(\frac{(2n+1)\pi}{b}\right)^2 - \left(\frac{(2m+1)\pi}{a}\right)^2} \cdot c'} \\ &\times \left[ i\sqrt{\frac{4\pi^2}{\lambda^2} - \left(\frac{(2n+1)\pi}{b}\right)^2 - \left(\frac{(2m+1)\pi}{a}\right)^2} \right. \\ &\left. + \left( ik - \frac{1}{R} \right) \sqrt{\cos^2 \alpha - \sin^2 \beta} \right] \\ &\times \int_0^b e^{-ik \sin \alpha \cdot x'} \sin \frac{(2n+1)\pi}{b} x' dx' \int_0^a e^{-ik \sin \beta \cdot y'} \\ &\times \sin \frac{(2m+1)\pi}{a} y' dy'. \end{aligned} \quad (34)$$

Substituting Equation (34) into Equation (28), one can get

$$\begin{aligned} \vec{\Phi}(x, y, z; t) &= -\frac{e^{ikR}}{4\pi R} e^{-i\omega t} \sum_{j=x, y, z} \sum_{m=0}^{\infty} \sum_{n=0}^{\infty} \frac{16A_j}{(2m+1)(2n+1)\pi^2} \\ &\times e^{i\sqrt{\frac{4\pi^2}{\lambda^2} - \left(\frac{(2n+1)\pi}{b}\right)^2 - \left(\frac{(2m+1)\pi}{a}\right)^2} \cdot c'} \\ &\times \left[ i\sqrt{\frac{4\pi^2}{\lambda^2} - \left(\frac{(2n+1)\pi}{b}\right)^2 - \left(\frac{(2m+1)\pi}{a}\right)^2} \right. \\ &\left. + \left( ik - \frac{1}{R} \right) \sqrt{\cos^2 \alpha - \sin^2 \beta} \right] \\ &\times \int_0^b e^{-ik \sin \alpha \cdot x'} \sin \frac{(2n+1)\pi}{b} x' dx' \int_0^a e^{-ik \sin \beta \cdot y'} \\ &\times \sin \frac{(2m+1)\pi}{a} y' dy' \vec{e}_j. \end{aligned} \quad (35)$$

Equation (35) is the total diffraction wave function in the diffraction area. From the wave function, we can obtain the diffraction intensity  $I$  on the display screen, we have

$$I \propto \left| \vec{\Phi}(x, y, z; t) \right|^2. \quad (36)$$

#### 4. Multiple-slit diffraction wave function of light

From Equation (23), in the first slit, the photon wave function  $\vec{\psi}_1(x, y, z; t)$  is

$$\begin{aligned} \vec{\psi}_1(x, y, z; t) &= \sum_{j=x, y, z} \sum_{m, n=0}^{\infty} \frac{16A_j}{(2m+1)(2n+1)\pi^2} \\ &\times \sin \frac{(2n+1)\pi x}{b} \sin \frac{(2m+1)\pi y}{a} \\ &\times e^{i\sqrt{\frac{4\pi^2}{\lambda^2} - \frac{(2n+1)^2 \pi^2}{b^2} - \frac{(2m+1)^2 \pi^2}{a^2}} z} e^{-i\omega t} \vec{e}_j. \end{aligned} \quad (37)$$

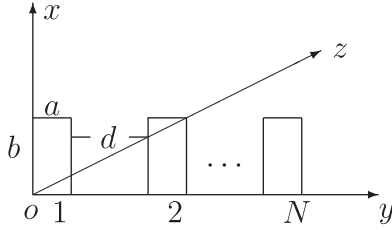


Figure 3. Multiple-slit geometry with  $a$  the single slit width,  $b$  the slit length and  $d$  the distance between the two slits.

From Figure 3, in the second slit, when we make the coordinate translations:

$$\begin{aligned} x' &= x \\ y' &= y - (a + d) \\ z' &= z, \end{aligned} \quad (38)$$

we can obtain the second slit photon wave function by the first slit photon wave function. It is

$$\begin{aligned} \vec{\psi}_2(x, y, z; t) &= \sum_{j=x, y, z} \sum_{m, n=0}^{\infty} \frac{16A_j}{(2m+1)(2n+1)\pi^2} \\ &\times \sin \frac{(2n+1)\pi x}{b} \sin \frac{(2m+1)\pi [y - (a+d)]}{a} \\ &\times e^{i\sqrt{\frac{4\pi^2}{\lambda^2} - \frac{(2n+1)^2\pi^2}{b^2} - \frac{(2m+1)^2\pi^2}{a^2}}z} e^{-i\omega t} \vec{e}_j. \end{aligned} \quad (39)$$

Similarly, we can also obtain the  $N$ th photon wave function. It is

$$\begin{aligned} \vec{\psi}_N(x, y, z; t) &= \sum_{j=x, y, z} \sum_{m, n=0}^{\infty} \frac{16A_j}{(2m+1)(2n+1)\pi^2} \sin \frac{(2n+1)\pi x}{b} \\ &\times \sin \frac{(2m+1)\pi [y - (N-1)(a+d)]}{a} \\ &\times e^{i\sqrt{\frac{4\pi^2}{\lambda^2} - \frac{(2n+1)^2\pi^2}{b^2} - \frac{(2m+1)^2\pi^2}{a^2}}z} e^{-i\omega t} \vec{e}_j. \end{aligned} \quad (40)$$

With Kirchhoff's law, similar to Equation (35), we can get the light diffraction wave function in every slit, these are

$$\begin{aligned} \vec{\Phi}_1(x, y, z; t) &= -\frac{e^{ikR}}{4\pi R} e^{-i\omega t} \sum_{j=x, y, z} \sum_{m=0}^{\infty} \sum_{n=0}^{\infty} \frac{16A_j}{(2m+1)(2n+1)\pi^2} \\ &\times e^{i\sqrt{\frac{4\pi^2}{\lambda^2} - \frac{(2n+1)\pi^2}{b^2} - \frac{(2m+1)\pi^2}{a^2}} \cdot c'} \\ &\times \left[ i\sqrt{\frac{4\pi^2}{\lambda^2} - \left(\frac{(2n+1)\pi}{b}\right)^2 - \left(\frac{(2m+1)\pi}{a}\right)^2} \right. \\ &\quad \left. + \left(ik - \frac{1}{R}\right) \sqrt{\cos^2 \alpha - \sin^2 \beta} \right] \\ &\times \int_0^b e^{-ik \sin \alpha \cdot x'} \sin \frac{(2n+1)\pi}{b} x' dx' \int_0^a e^{-ik \sin \beta \cdot y'} \\ &\times \sin \frac{(2m+1)\pi}{a} y' dy' \vec{e}_j. \end{aligned} \quad (41)$$

$$\begin{aligned} \vec{\Phi}_2(x, y, z; t) &= -\frac{e^{ikR}}{4\pi R} e^{-i\omega t} \sum_{j=x, y, z} \sum_{m=0}^{\infty} \sum_{n=0}^{\infty} \frac{16A_j}{(2m+1)(2n+1)\pi^2} \\ &\times e^{i\sqrt{\frac{4\pi^2}{\lambda^2} - \frac{(2n+1)\pi^2}{b^2} - \frac{(2m+1)\pi^2}{a^2}} \cdot c'} \\ &\times \left[ i\sqrt{\frac{4\pi^2}{\lambda^2} - \left(\frac{(2n+1)\pi}{b}\right)^2 - \left(\frac{(2m+1)\pi}{a}\right)^2} \right. \\ &\quad \left. + \left(ik - \frac{1}{R}\right) \sqrt{\cos^2 \alpha - \sin^2 \beta} \right] \\ &\times \int_0^b e^{-ik \sin \alpha \cdot x'} \sin \frac{(2n+1)\pi}{b} x' dx' \\ &\times \int_{a+d}^{2a+d} e^{-ik \sin \beta \cdot y'} \sin \frac{(2m+1)\pi}{a} y' dy' \vec{e}_j. \end{aligned} \quad (42)$$

$$\begin{aligned} \vec{\Phi}_N(x, y, z; t) &= -\frac{e^{ikR}}{4\pi R} e^{-i\omega t} \sum_{j=x, y, z} \sum_{m=0}^{\infty} \sum_{n=0}^{\infty} \frac{16A_j}{(2m+1)(2n+1)\pi^2} \\ &\times e^{i\sqrt{\frac{4\pi^2}{\lambda^2} - \frac{(2n+1)\pi^2}{b^2} - \frac{(2m+1)\pi^2}{a^2}} \cdot c'} \\ &\times \left[ i\sqrt{\frac{4\pi^2}{\lambda^2} - \left(\frac{(2n+1)\pi}{b}\right)^2 - \left(\frac{(2m+1)\pi}{a}\right)^2} \right. \\ &\quad \left. + \left(ik - \frac{1}{R}\right) \sqrt{\cos^2 \alpha - \sin^2 \beta} \right] \\ &\times \int_0^b e^{-ik \sin \alpha \cdot x'} \sin \frac{(2n+1)\pi}{b} x' dx' \\ &\times \int_{(N-1)(a+d)}^{(N-1)(a+d)+a} e^{-ik \sin \beta \cdot y'} \sin \frac{(2m+1)\pi}{a} y' dy' \vec{e}_j. \end{aligned} \quad (43)$$

The total diffraction wave function for the  $N$ th-slit is

$$\begin{aligned} \vec{\Phi}(x, y, z; t) &= \vec{\Phi}_1(x, y, z; t) + \vec{\Phi}_2(x, y, z; t) + \dots \\ &\quad + \vec{\Phi}_N(x, y, z; t). \end{aligned} \quad (44)$$

From Equation (44), we can obtain the diffraction intensity  $I$  on the display screen for the  $N$ th-slit, so we have

$$I \propto |\vec{\Phi}(x, y, z; t)|^2. \quad (45)$$

When  $b \rightarrow \infty$ , we can get the single-slit light diffraction wave function

$$\begin{aligned} \vec{\Phi}_{b \rightarrow \infty}(y, z; t) &= -\frac{e^{ikR}}{4\pi R} e^{-i\omega t} \sum_{j=x, y, z} \sum_{m=0}^{\infty} \frac{4A_j}{(2m+1)\pi} e^{i\sqrt{\frac{4\pi^2}{\lambda^2} - \frac{(2m+1)\pi^2}{a^2}} \cdot c'} \\ &\times \left[ i\sqrt{\frac{4\pi^2}{\lambda^2} - \left(\frac{(2m+1)\pi}{a}\right)^2} + \left(ik - \frac{1}{R}\right) \sqrt{\cos^2 \alpha - \sin^2 \beta} \right] \\ &\times \int_0^a e^{-ik \sin \beta \cdot y'} \sin \frac{(2m+1)\pi}{a} y' dy' \vec{e}_j. \end{aligned} \quad (46)$$



From Equation (46), we can obtain the diffraction intensity  $I_{b \rightarrow \infty}$  on the display screen for single-slit when  $b \rightarrow \infty$ . It is

$$I_{b \rightarrow \infty} \propto |\vec{\Phi}_{b \rightarrow \infty}(y, z, t)|^2. \quad (47)$$

In [11], the authors had first studied light diffraction with the old quantum theory, i.e. the quantum mechanics of the correspondence principle. They had considered a quantum of light entering a three-dimensional crystal lattice, and calculated the light momentum loss after collision, with the quantization condition and the light quantum momentum formula  $p = \frac{h}{\lambda}$ . They obtained the relation between the deflecting angle of the light quantum collision with the lattice and the lattice period. By analyzing this, the authors given the expression of electronic density distributed on the grating  $\rho = A_m \sin \frac{2\pi mx}{a}$ . The coefficient  $A_m$  could be obtained by Fourier analysis. The diffraction spectrum intensity of the  $m$ th order is proportional to  $A_m^2$ . Finally, they obtained the intensity formula of the diffraction spectrum, which was in complete agreement with the classical diffraction. The formula gives a simple relation between diffraction intensity, slit width, wavelength of incident light and diffraction angle. In this paper, we present the quantum theory of light diffraction using the framework of a relativistic quantum theory, and obtain the relation between the diffraction intensity, slit length, slit width, slit thickness, light wavelength and diffraction angle. Through calculation, we find the theoretical results are in accordance with the experimental data, and give some new theory predictions.

## 5. Numerical results

The light diffraction experiment of single and multiple slits was reported by H.F. Neiners in 1970 [14]. In the experiment [14], the optical system consisted of two convex lenses, the focal length  $f$ , a diffraction screen of slit length  $b$  and slit width  $a$  ( $b \gg a$ ) and a display screen. The laser light source of wavelength  $\lambda$  is placed on the focal plane of the first convex lens, the first lens makes the light beams parallel and incident on the diffraction screen, the second lens is next to the diffraction screen, and the display screen is placed on the focal plane of second convex lens. In the experiment, the diffraction patterns were shown by photographs, but experimental data were not given. The author found his results could be explained excellently by the classical theoretical formula. It is

$$I = I_0 \frac{\sin^2 \beta \sin^2 N\gamma}{\beta^2 \sin^2 \gamma}, \quad (48)$$

where

$$\beta = \frac{a\pi \sin \theta}{\lambda}, \quad \gamma = \frac{(a+d)\pi \sin \theta}{\lambda}, \quad (49)$$

$\theta$  is the diffraction angle,  $a$  is the width of slit,  $d$  is the distance from the first slit to the second slit, and  $n$  is the number of slits.

Figure 4(a)–(f) shows the diffraction patterns from two, three, four, five, six and seven slits with  $\lambda = 6.328 \times 10^{-7}$  m, the slit width  $a = 0.88 \times 10^{-4}$  m,  $a + d = 3.52 \times 10^{-4}$  m ( $d$  is the distance between two slits), and the distance between slit and display screen  $R = 4.572$  m. In Figure 4(a)–(f), the solid curve is our theoretical result, and the dotted curve is the result of Equation (48), i.e. the diffraction data. In Figure 4(a)–(f), we use the same experimental parameters in our calculation, and the theoretical input parameters are: slit length  $b = 3.52 \times 10^{-4}$  m, and slit thickness  $c' = 0.88 \times 10^{-4}$  m. From Figure 4(a), we can find the calculation result is in accordance with experimental data. Since the ratio  $\frac{a+d}{a} = 4$ , we find the orders 4, 8, 12 ... are missing. The conclusion is accordance with classical optics.

Figure 4(b)–(f) are multiple slits diffraction patterns corresponding to slit number  $N=3, 4, 5, 6, 7$ . We can find the calculation results are in accordance with experiment data, and there are  $N-2$  secondary maxima and  $N-1$  minima between the two principle maxima. The conclusions are accordance with classical optics.

Figure 5 shows the diffraction patterns for the single slit. In the experiment, the light wavelength  $\lambda = 6.328 \times 10^{-7}$  m, the slit width  $a = 1.76 \times 10^{-4}$  m, and the distance between the slit and display screen  $R = 4.572$  m. In our calculation, we take the same experimental parameters above, and the theoretical input parameters are: slit length  $b = 4.0 \times 10^{-4}$  m, the slit thickness  $c' = 1.1 \times 10^{-6}$  m, and the diffraction angle  $\alpha = 0.001$  rad. In Figure 5, the solid curve is our theoretical result and the dotted curve is the result of Equation (48), i.e. the diffraction data. From Figure 5, we find the calculation result shows good agreement with experimental data. We have compared the theoretical results with the experiment data above. In the following, we give some theoretical predictions. In the calculations, we take the light wavelength to be  $\lambda = 6.328 \times 10^{-7}$  m, the distance  $R = 4.572$  m and the diffraction angle  $\alpha = 0.001$  rad.

Figure 6 is obtained by taking the single slit width as  $5a$ ,  $10a$  and  $20a$  ( $a = 1.76 \times 10^{-4}$  m) and  $b = 4.0 \times 10^{-4}$  m,  $c' = 1.1 \times 10^{-6}$  m. From Figure 6, we find that when the slit width increases, the diffraction patterns become narrower, and the diffraction intensity increases.

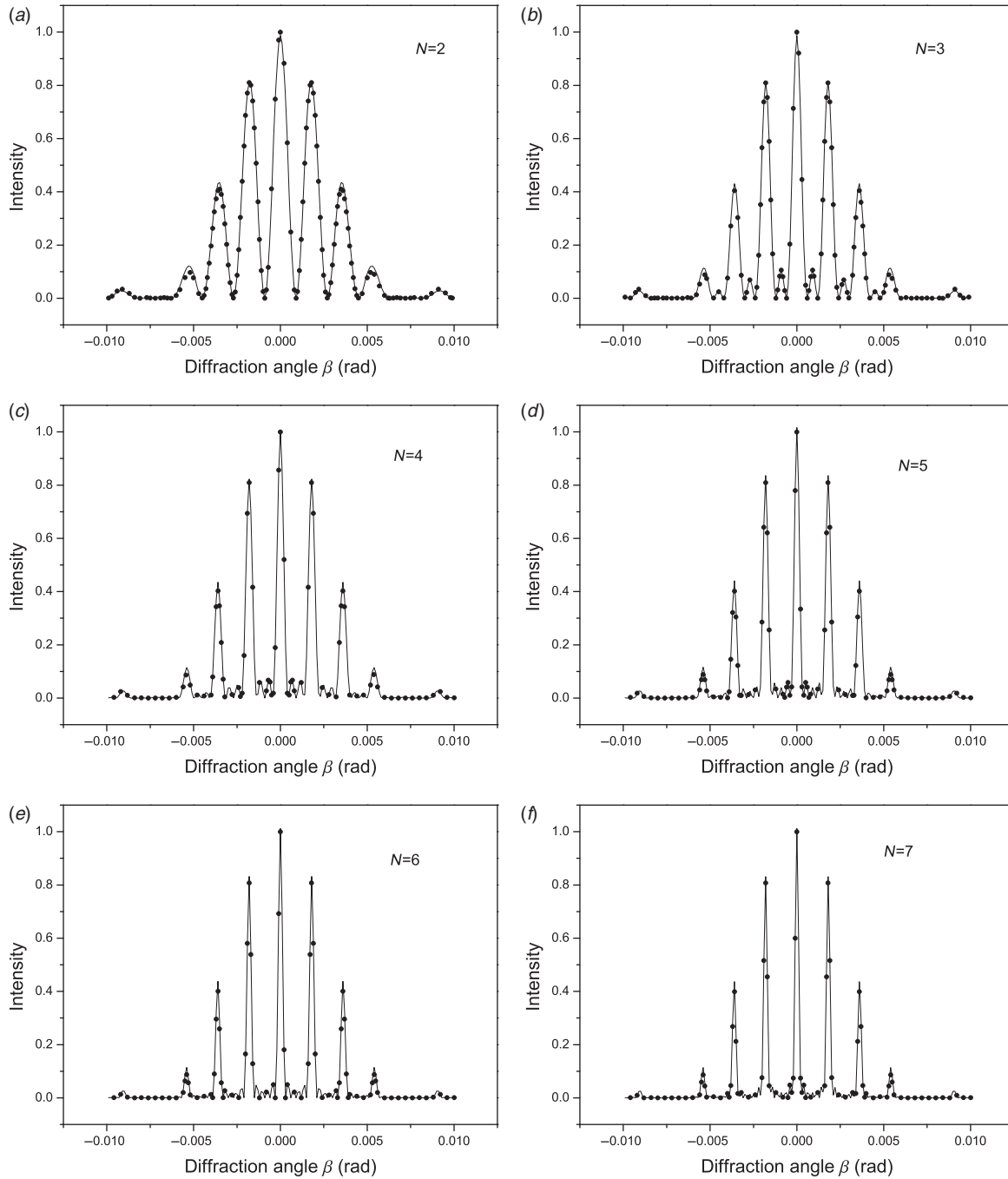


Figure 4. The diffraction patterns from two, three, four, five, six and seven slits with  $a = 0.88 \times 10^{-4} \text{ m}$ ,  $a + d = 3.52 \times 10^{-4} \text{ m}$ ,  $b = 4 \times 0.88 \times 10^{-4} \text{ m}$ ,  $c' = 0.88 \times 10^{-4} \text{ m}$ . The solid curve is our theoretical calculations and the dot curve is the result of Equation (48).

In Figure 7, the slit width and slit length are equal ( $a = b$ ), and this is obtained by taking the slit length and slit width as  $\lambda$ ,  $3\lambda$  and  $5\lambda$ , and  $c' = 1.1 \times 10^{-6} \text{ m}$ . From Figure 7, we can find that when they increase, the diffraction patterns become narrower, and the diffraction intensity increases.

In Figure 8, we obtain an important result: when  $a = b \leq 0.1\lambda$ , the total diffraction intensity is zero,

i.e. a very small hole cannot produce diffraction phenomenon. This is because the incident light scatters back completely when the size of slit is very small.

Figure 9 is obtained by taking the single slit length as  $50b$ ,  $70b$  and infinity ( $b = 4.0 \times 10^{-4} \text{ m}$ ) and  $a = 1.76 \times 10^{-4} \text{ m}$ ,  $c' = 1.1 \times 10^{-6} \text{ m}$ . From Figure 9, we can obtain the following conclusions. (1) When the slit length increases, the diffraction intensity increases.



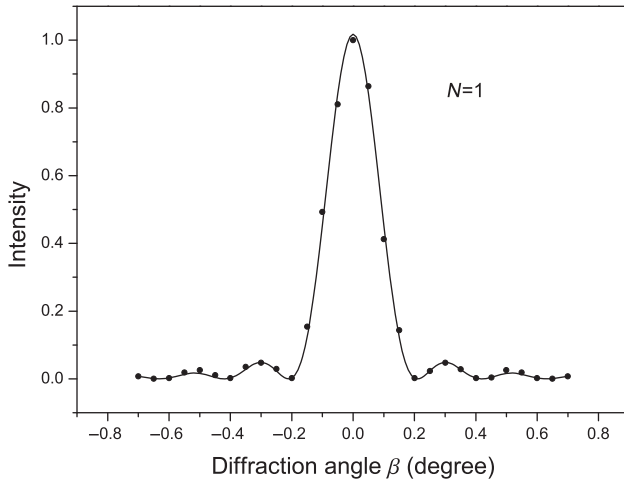


Figure 5. The diffraction patterns from single slit  $a = 1.76 \times 10^{-4}$  m,  $b = 4.0 \times 10^{-4}$  m and  $c' = 1.1 \times 10^{-6}$  m. The solid curve is our theoretical results and the dot curve is the result of Equation (48).

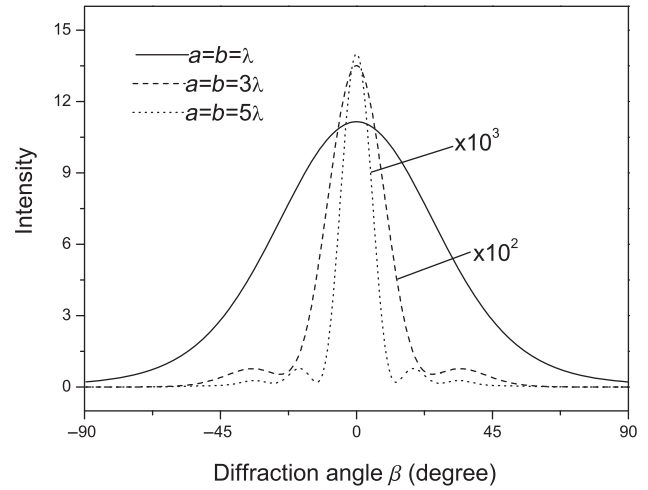


Figure 7. The diffraction patterns from single slit with  $c' = 1.1 \times 10^{-6}$  m. The solid, dash and dot curves correspond to  $a = b = \lambda$ ,  $a = b = 3\lambda$  and  $a = b = 5\lambda$ .

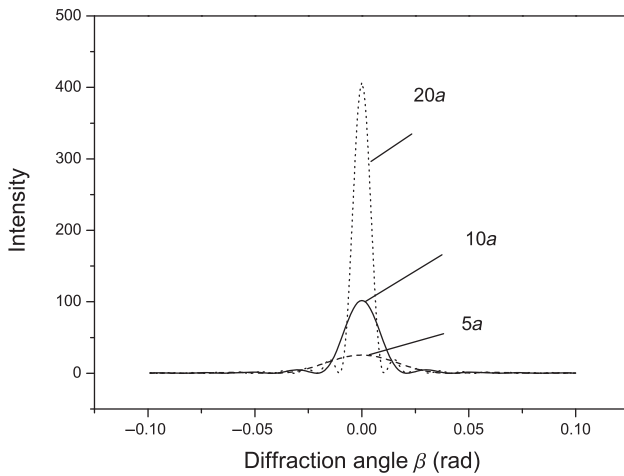


Figure 6. The diffraction patterns from single slit with  $b = 4.0 \times 10^{-4}$  m and  $c' = 1.1 \times 10^{-6}$  m. The dash, solid and dot curves correspond to slit width  $5a$ ,  $10a$  and  $20a$  ( $a = 1.76 \times 10^{-4}$  m), respectively.

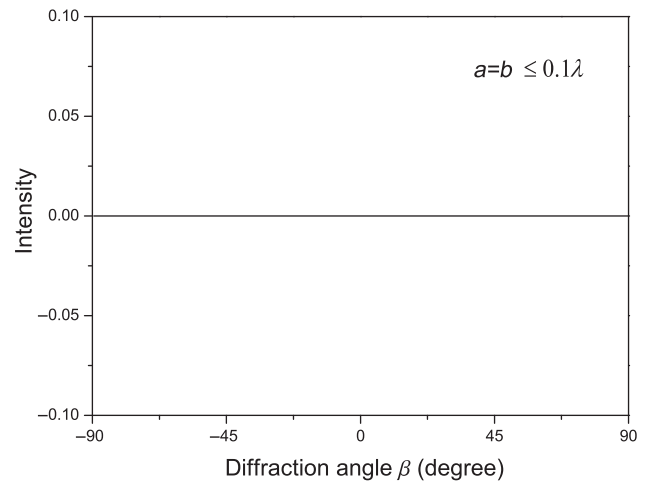


Figure 8. The diffraction patterns from single slit with  $c' = 1.1 \times 10^{-6}$  m and  $a = b \leq 0.1\lambda$ . Their real intensity  $I$  should be multiplied by  $10^2$  and  $10^3$ .

(2) When the slit length changes, the width of the diffraction patterns does not change.

Figure 10 is obtained by taking the single slit thickness as  $100c'$ ,  $1000c'$ ,  $2000c'$  and  $3000c'$  ( $c' = 1.1 \times 10^{-6}$  m) and  $a = 1.76 \times 10^{-4}$  m,  $b = 4.0 \times 10^{-4}$  m. From Figure 10, we can obtain the following conclusions: (1) when the slit thickness increases, the total diffraction intensity decreases; (2) when the slit thickness increases, the diffraction patterns are spread over a wide area.

Figure 11 is obtained by taking the single wavelength as  $10\lambda$ ,  $20\lambda$  and  $50\lambda$  ( $\lambda = 6.328 \times 10^{-7}$  m)

and  $a = 1.76 \times 10^{-4}$  m,  $b = 4.0 \times 10^{-4}$  m,  $c' = 1.1 \times 10^{-6}$  m. From Figure 11, we can obtain the following conclusions: (1) when the wavelength decreases, the total diffraction intensity increases and the diffraction patterns become narrow; (2) when the wavelength decreases, the number of diffraction patterns increases.

Figure 12 is obtained by taking the double slit thickness as  $c'$ ,  $10c'$  and  $50c'$  ( $c' = 0.88 \times 10^{-4}$  m) and  $a = 0.88 \times 10^{-4}$  m,  $b = 4 \times 0.88 \times 10^{-4}$  m,  $a + d = 3.52 \times 10^{-4}$  m. From Figure 12, we can obtain the following conclusions: (1) when the slit thickness increases, the diffraction intensity decreases;

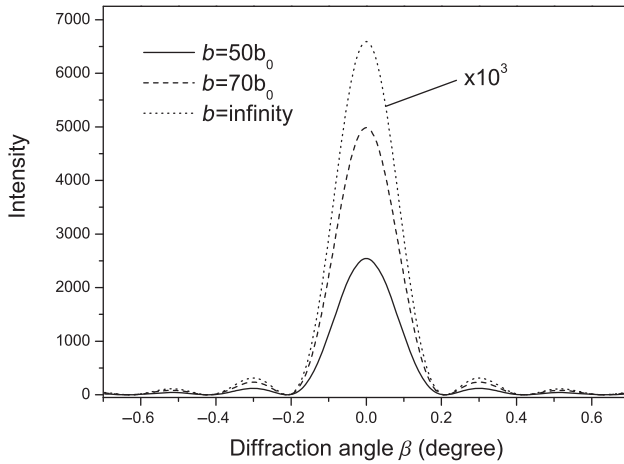


Figure 9. The diffraction patterns from single slit with  $a = 1.76 \times 10^{-4}$  m and  $c' = 1.1 \times 10^{-6}$  m. The solid, dash and dot curves correspond to slit length  $50b_0$ ,  $70b_0$  and infinity ( $b_0 = 4.0 \times 10^{-4}$  m), respectively.

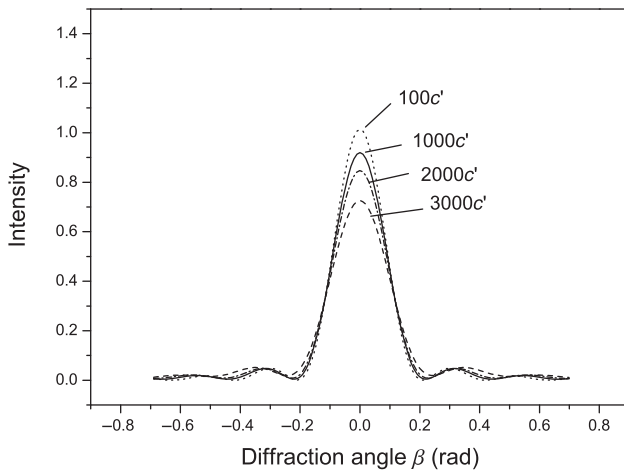


Figure 10. The diffraction patterns from single slit with  $a = 1.76 \times 10^{-4}$  m and  $b = 4.0 \times 10^{-4}$  m. The dot, solid, dash-dot and dash curves correspond to slit thickness  $100c'$ ,  $1000c'$ ,  $2000c'$  and  $3000c'$  ( $c' = 1.1 \times 10^{-6}$  m), respectively.

(2) in classical optics, we know when the ratio  $\frac{a+d}{a} = n$  ( $n = 1, 2, 3, \dots$ ), the orders  $n, 2n, 3n, \dots$  are missing in double slit diffraction. We find that when the slit thickness takes  $c'$ , and the ratio  $\frac{a+d}{a} = 4$ , the orders 4, 8, 12, ... are missing. (3) When the slit thickness increases, such as  $10c'$  and  $50c'$ , we find the missing-order phenomenon disappears.

From Figures 4 and 5, we can find our calculation results are in accordance with the experimental data, the classical optics results and the old quantum theory results [13]. From Figures 6 to 12, we give some new predictions, which can be tested by light diffraction experiments.

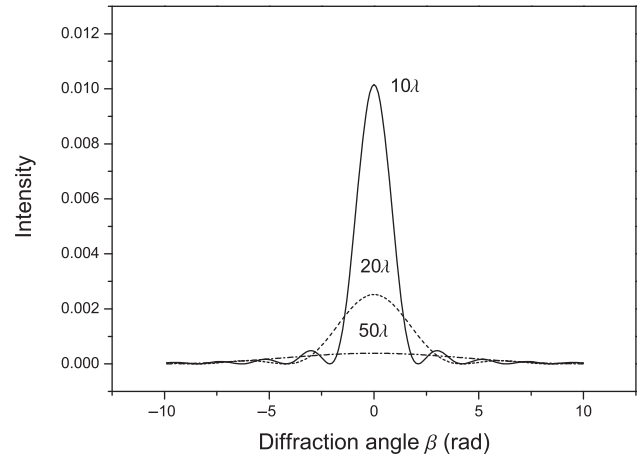


Figure 11. The diffraction patterns from single slit with  $a = 1.76 \times 10^{-4}$  m,  $b = 4.0 \times 10^{-4}$  m and  $c' = 1.1 \times 10^{-6}$  m. The solid, dash and dash-dot curves correspond to wave-lengths  $10\lambda$ ,  $20\lambda$  and  $50\lambda$ .

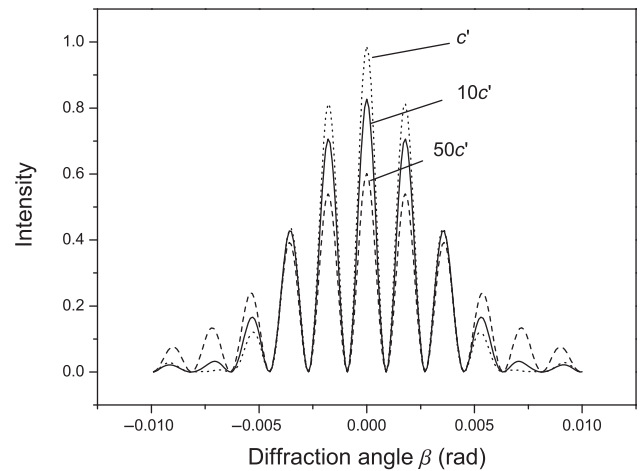


Figure 12. The diffraction patterns from double slit with  $a = 0.88 \times 10^{-4}$  m,  $b = 4 \times 0.88 \times 10^{-4}$  m and  $a + d = 3.52 \times 10^{-4}$  m. The dot, solid and dash curves correspond to slit thickness  $c'$ ,  $10c'$  and  $50c'$ .

## 6. Conclusion

In conclusion, we have studied the single-slit, double-slit and multiple-slit diffraction of light with the relativistic quantum mechanical approach. We give the relation between diffraction intensity, slit length, slit width, slit thickness, wavelength of light and diffraction angle. Our calculation results are in accordance with the experiment data of the single-slit, double-slit and multiple-slit diffraction. In addition, we study the effect of slit length, slit width, slit thickness, the wavelength of light on the diffraction intensity and form of diffraction pattern. The effect of slit length and

slit thickness on the diffraction pattern cannot be obtained in classical optics. In double slit diffraction, we find when the ratio  $\frac{a+d}{a} = n$  ( $n=1, 2, 3 \dots$ ), the orders  $n, 2n, 3n, \dots$  are missing. When the slit thickness increases, the missing order phenomenon disappears. In multiple slit diffraction, we find there are  $N-2$  secondary maxima and  $N-1$  minima between the two principle maxima, we think that all the new predictions in our work can be tested by light diffraction experiments.

## References

- [1] Ghosh, R.; Mandel, L. *Phys. Rev. Lett.* **1987**, *59*, 1903–1905.
- [2] Strekalov, D.V.; Sergienko, A.V.; Klyshko, D.N.; Shih, Y.H. *Phys. Rev. Lett.* **1995**, *74*, 3600–3603.
- [3] Pittman, T.B.; Shih, Y.H.; Strekalov, D.V.; Sergienko, A.V. *Phys. Rev. A* **1995**, *52*, R3429–R3432.
- [4] Hanbury Brown, R.; Twiss, R.Q. *Nature* **1956**, *178*, 1046–1048.
- [5] Haner, A.B.; Isenor, N.R. *Am. J. Phys.* **1970**, *38*, 748–751.
- [6] Zhai, Y.-H.; Chen, X.-H.; Zhang, D.; Wu, L.-A. *Phys. Rev. A* **2005**, *72*, 043805.
- [7] Pfleegor, R.I.; Mandel, L. *Phys. Rev.* **1967**, *159*, 1084–1088; Ou, Z.Y.; Gage, E.C.; Magill, B.E.; Mandel, L. *Opt. Commun.* **1988**, *69*, 1–5.
- [8] Gatti, A.; Brambilla, E.; Bache, M.; Lugiato, L.A. *Phys. Rev. Lett.* **2004**, *93*, 093620; Ferri, F.; Magatti, D.; Gatti, A.; Bache, M.; Brambilla, E.; Lugiato, L.A. *Phys. Rev. Lett.* **2005**, *94*, 183602.
- [9] Bennink, R.S.; Bentley, S.J.; Boyd, R.W. *Phys. Rev. Lett.* **2002**, *89*, 113601.
- [10] Scarcelli, G.; Valencia, A.; Shih, Y. *Phys. Rev. A* **2004**, *70*, 051802(R); D'Angelo, M.; Valencia, A.; Rubin, M.H.; Shih, Y. *Phys. Rev. A* **2005**, *72*, 013810.
- [11] Epstein, P.S.; Ehrenfest, P. *Proc. Nat. Acad. Sci.* **1924**, *10*, 133–139.
- [12] Smith, B.J.; Raymer, M.G. *New J. Phys.* **2007**, *9*, 414.
- [13] Schwartz, M. *Principles of Electrodynamics*; Oxford University Press: Oxford, 1972.
- [14] Meiners, H.F. *Physics Demonstration Experiments*; The Ronald Press: New York, 1970; Vol. II.